

amplitude may be compared with other recent experimental determinations.<sup>4,6,19</sup> A curve calculated from the dispersion relations by Salzman and Schnitzer<sup>5</sup> is chosen for comparison in Fig. 6. It can be seen that the values obtained in this experiment are in statistical agreement with the values calculated from the dispersion relations. The change between the present experiment and the earlier results of the Carnegie group<sup>4</sup> is due primarily to the increase in total cross section.

<sup>19</sup> Barnes, Rose, Giacomelli, Ring, and Miyake (private communication).

The largest single uncertainty in this experiment is the fraction of  $\mu$  mesons and electrons in the incident beam. An improved technique for determining this fraction would clearly be desirable for future experiments in this energy region.

#### ACKNOWLEDGMENTS

We wish to thank John Lathrop for his help in the preparation of the experiments. The assistance of many people, in particular John Lathrop, Robert March, and Luciano Tau, in running the experiment and taking data is gratefully acknowledged.

### Scattering of $\mu$ Mesons from Lead Nuclei\*

B. CHIDLEY, P. GOLDSTEIN,† G. HINMAN, R. SUMMERS, AND R. ADLER

*Department of Physics, Carnegie Institute of Technology, Pittsburgh, Pennsylvania*

(Received June 22, 1959)

The angular distribution of 23-Mev  $\mu^-$  mesons scattered by lead nuclei has been measured by using a counter arrangement and also by using a propane bubble chamber. The results agree, to the accuracy of the experiments, with the distribution predicted by the ordinary Coulomb interaction of the  $\mu$  meson and the lead nucleus.

#### INTRODUCTION

FOR many years the interactions of the  $\mu$  meson with matter have been the subject of experimental investigations.

Measurements<sup>1</sup> on  $\mu$ -mesonic atoms, on the production of stars by energetic muons, and on the creation of muon pairs by gamma rays have revealed an interaction between the muon and the electromagnetic field that is compatible with the assumption that the muon behaves in the same way as an electron except that it has a larger mass. More recent measurements have established that the magnetic dipole moment has the expected value<sup>2</sup> and that there is no evidence for a parity violating interaction of the electric dipole type.<sup>3</sup> The strength of the nuclear interaction has been established by a study of the lifetimes of negative muons in numerous materials,<sup>1</sup> and the result is that this interaction is of the "weak" type. All of these results lead to the conclusion that the  $\mu$  meson has interactions that are well understood.

\* Research supported by the U. S. Atomic Energy Commission.

† Now at Princeton University, Princeton, New Jersey. This work submitted in partial fulfillment of the requirements for the degree of Doctor of Philosophy at Carnegie Institute of Technology.

<sup>1</sup>  $\mu$ -meson physics has been summarized recently by J. Rainwater, *Annual Review of Nuclear Science* (Annual Reviews, Inc., Palo Alto, 1957), Vol. 7, p. 1.

<sup>2</sup> Coffin, Garwin, Lederman, Penman, and Sachs, *Phys. Rev.* **106**, 1108–1110 (1957).

<sup>3</sup> Berley, Garwin, Gidal, and Lederman, *Bull. Am. Phys. Soc.* **4**, 81 (1959).

One series of experiments on the  $\mu$  meson, however, has not uniformly given results in accord with the interactions mentioned above. These are the experiments on the elastic scattering of muons from nuclei. Several experiments<sup>4</sup> have confirmed the simple interpretation of the scattering in terms of the Coulomb interaction, but several other investigations<sup>5</sup> have revealed an excess of large-angle scatterings over the number expected.

All of these experiments have been carried out using cosmic-ray  $\mu$  mesons. The beams obtainable from this source are very weak and polychromatic. The experiment described in this paper<sup>6</sup> utilized a  $\mu$ -meson beam from an accelerator, the 450-Mev synchrocyclotron at Carnegie Institute of Technology. The beam was more intense and monoenergetic than cosmic rays can provide, but the energy was much lower, about 23 Mev. At such a low energy the scattered  $\mu$  mesons detected in the experiment did not appreciably penetrate the nucleus. Although it would seem most probable that an anomaly, if it does indeed exist, would arise from an interaction of a relatively short range, never-

<sup>4</sup> Amaldi, Fidecaro, and Mariani, *Nuovo cimento* **7**, 553 (1950); Kirillov-Ugriumov, Dolgoshien, Moskvichov, and Morozova, *J. Exptl. Theoret. Phys. U.S.S.R.* **36**, 415 (1959) [translation: *Soviet Phys. JETP* **36**(9) 290 (1959)]; Fukui, Kitamura, and Watase, *Phys. Rev.* **113**, 315 (1959).

<sup>5</sup> Lloyd, Rössle, and Wolfendale, *Proc. Phys. Soc. (London)* **A70**, 421 (1957); this article summarizes most of the early work.

<sup>6</sup> A preliminary report on this work was published [B. Chidley *et al.* *Can. J. Phys.* **36**, 801 (1958)].

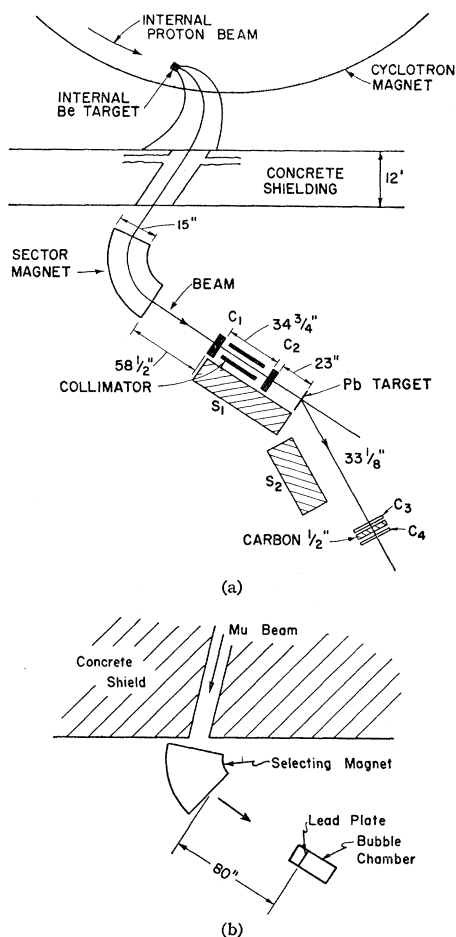


FIG. 1. (a) Experimental setup for counter experiment. (b) Experimental setup for bubble chamber experiment.

theless the experiments described in paragraph two above give no more reason to exclude a longer range anomalous force than a shorter range one. Perhaps the situation would be better stated by saying that the experiments provide as much evidence against the presence of any anomalous short-range interaction as against the presence of a longer range one. The present study of  $\mu$ -meson scattering was carried out using two separate experimental techniques, one involving a bubble chamber and the other a counter setup. The systematic errors involved in the two should be quite different and a comparison of the results should help to reveal whether such errors have been eliminated.

#### BEAM

The  $\mu$ -meson beam used in the experiment was obtained in the way shown in Fig. 1 and described below. The circulating proton beam in the C.I.T. synchrocyclotron was allowed to strike an internal beryllium target producing  $\pi$  mesons. Many of these mesons decayed in the vicinity of the target providing a rather diffuse source of negative  $\mu$  mesons in the

target area. The magnetic field of the cyclotron provided separation of these muons into a fanshaped beam, each portion of which had a somewhat peaked momentum distribution. A portion of this beam was allowed to pass through a collimating hole in the shielding wall around the cyclotron and into a sector magnet. The magnet gave additional momentum selection and was adjusted so that  $37 \pm 2.2$  Mev muons were deflected toward the scattering apparatus. The center of the momentum spectrum selected was 95 Mev/c.

This beam was analyzed into its individual components by taking a differential range curve using counters and was found to consist of  $\mu$  mesons (25%),  $\pi$  mesons (5%), and electrons (70%). The beam intensity was 3500 muons/min over a five-inch diameter circle at a distance of 115 inches from the magnet face.

#### BUBBLE CHAMBER EXPERIMENT

A propane bubble chamber was used to study the  $\mu$ -meson scattering. It was 2 in.  $\times$  3 in.  $\times$  6 in. in size and was oriented so that the meson beam entered it through a  $\frac{3}{8}$ -in. stainless steel window in one of the 2-in.  $\times$  3-in. faces and traveled along the 6-in. length. A 0.22-in.  $\times$  2-in.  $\times$  3-in. lead foil, held by a Lucite frame, was placed in the chamber about  $1\frac{3}{4}$  in. from the window and comprised the scattering target for the  $\mu$  mesons. Scattering events were photographed stereoscopically through one of the hercullite windows by the light from a high-voltage flash tube mounted opposite the other window, as shown in Fig. 2. Figure 2 also shows surrounding the chamber the oven that was used to maintain it at its operating temperature of 138°F.

The pictures taken by the cameras were projected and measurements made on the scattered  $\mu$  mesons in the two stereoscopic views. Ninety percent of the

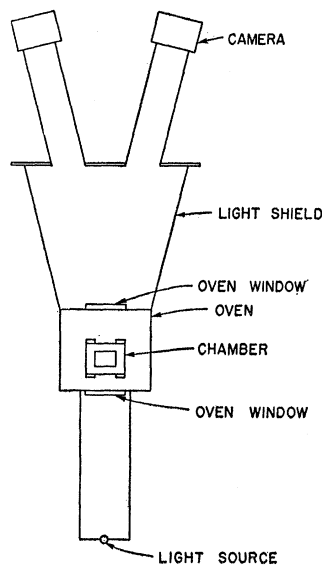


FIG. 2. Camera arrangement for bubble chamber experiment.

$\mu$ -meson tracks were easy to distinguish from those of other particles because of the decay electrons at the ends of them. From the measurements taken it was possible to compute (1) the space angle between the incident and scattered mu meson, (2) the range of the particle after scattering, and (3) the location of the scattering point and the end point of the track. For these calculations the number 1.25 was used for the index of refraction of the propane.

Using the methods described above, a differential range curve of the muon beam was obtained and is shown in Fig. 3. Only particles with ranges lying within the vertical dotted lines corresponding to energy limits of 21.5 Mev to 25.3 Mev were analyzed for the angular distribution. These energies are given for the  $\mu$  mesons when they have penetrated halfway through the lead plate. The energies of the mesons were calculated using the reports of Willis and Thompson<sup>7</sup> for propane and lead. The propane was considered to have expanded adiabatically and to have a density<sup>8</sup> of 0.42 g/cm<sup>3</sup>.

96 000<sup>9</sup> pictures with the lead plate and 5000 without the plate were obtained in 4.5 days running time. Most of the pictures obtained with the chamber were quite clear and easily scanned. Some typical events are shown in Fig. 4. Every 1000 pictures yielded about 150 usable events. All  $\mu$ -meson events satisfied the following criteria:

1. The particle entered the chamber through the front window.
2. After scattering, the particle stopped in that part of the chamber visible to both cameras and a decay electron was seen in both views.

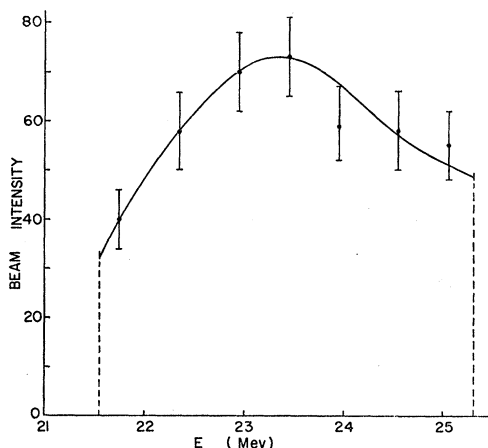


FIG. 3. Differential range curve of  $\mu$  mesons in bubble chamber.

<sup>7</sup> Beverly Hill Willis, University of California Radiation Laboratory Report UCRL-2426 (unpublished); T. J. Thompson, University of California Radiation Laboratory Report UCRL-1910 (unpublished).

<sup>8</sup> F. Din, *Thermodynamic Functions of Gases* (Butterworths Scientific Publications, London, 1956).

<sup>9</sup> Two views of an event are called one picture.

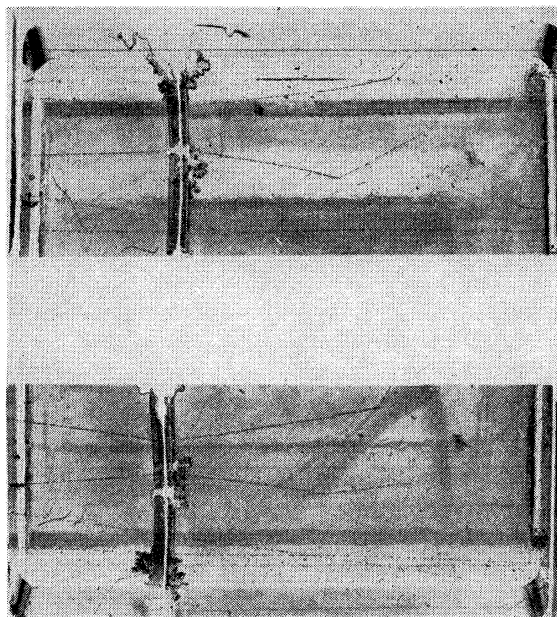


FIG. 4. Bubble chamber photographs of scattered  $\mu$  mesons.

It was necessary to correct the angular distribution obtained directly from the pictures in order to take account of scattered muons that did not satisfy the criteria for track acceptance. A particle of range  $R$  and scattering angle  $\theta$  might or might not have stopped in the chamber depending on the part of the lead plate it scattered from. Furthermore, a clamp that held the upper glass window in place obscured, for each camera view, a portion of the chamber. Because only those particles having the decay electron visible in both views were counted, it was necessary to multiply the observed distribution by a correction factor to obtain the actual number of particles that scattered into a particular angular range. Figure 5 gives the correction factor as a function of the scattering angle for the chamber used.

The error in cross section that would have been introduced if the pions in the beam were mistaken for muons has been calculated<sup>10</sup> and shown to be at most 0.5%. An electron could be mistaken for a muon if it suffered a large-angle nuclear scattering in the propane (thus looking like a muon giving rise to a decay electron) in the appropriate region of the chamber, that is between 2.1 and 2.8 inches from the lead plate. This effect has also been calculated<sup>10</sup> and found to be negligible.

The possibility that a muon was scattered from a portion of the herculite glass obscured by the plastic holder and was counted as a lead scattering has been considered and found to be less than 0.06% and is therefore negligible.

The procedure used in scanning the pictures was

<sup>10</sup> P. Goldstein, thesis, Carnegie Institute of Technology, 1958 (unpublished).

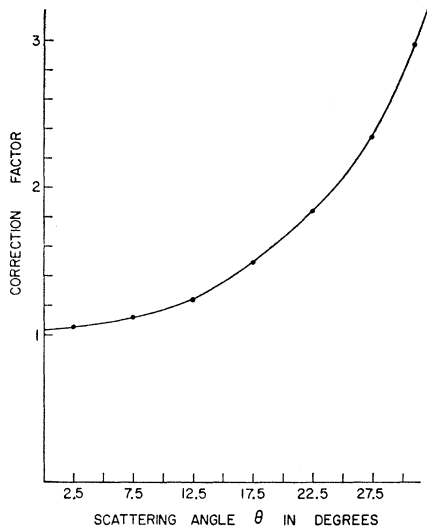


FIG. 5. Correction factor for bubble chamber experiment.

designed to eliminate the effects of scanner inefficiency. Inefficiency in this case is meant to denote the overlooking of a muon by a scanner or an inaccurate measurement on an event. All pictures were scanned independently by two persons at different times, and the results were compared. All events which, according to both measurements, fell into the same angular bin (the bins were  $0^\circ$ – $10^\circ$ ,  $10^\circ$ – $15^\circ$ ,  $15^\circ$ – $20^\circ$ ,  $20^\circ$ – $25^\circ$ ,  $25^\circ$ – $30^\circ$ ,  $30^\circ$ – $35^\circ$ ) were accepted. Events not in agreement and those seen by only one scanner were referred for a third scanning. The third scanning was done by a member of the experimental group. In any case of disagreement in the first two scannings, the result of the third scanning was accepted.

Even with this scanning procedure there will be some modification of the angular distribution of the scattered muons because of mismeasurements and it is important to estimate this correction. The assumption was made for the analysis that the probability of measuring a scattering angle  $\theta$ , when the actual angle is  $\Theta$ , has a Gaussian shape

$$P(\Theta, \theta) = (2\pi\sigma^2)^{-\frac{1}{2}} \exp[-(\theta - \Theta)^2/2\sigma^2].$$

The standard deviation of this Gaussian,  $\sigma$ , was determined for the scanners to be  $2.6^\circ$ . The probability, therefore, that a meson actually scattered at angle  $\Theta$

TABLE I. Comparison of bubble chamber experiment with theory.

Angular interval	$N_{\text{exp}}$	$N_{\text{th}}$	Ratio $N_{\text{exp}}/N_{\text{th}}$
0– $10^\circ$	$0.742 \pm 0.011$	0.729	$1.018 \pm 0.015$
10– $15^\circ$	$0.178 \pm 0.006$	0.191	$0.93 \pm 0.040$
15– $20^\circ$	$0.0538 \pm 0.0046$	0.0572	$0.94 \pm 0.07$
20– $25^\circ$	$0.0153 \pm 0.0015$	0.0128	$1.20 \pm 0.11$
25– $30^\circ$	$0.0067 \pm 0.0011$	0.00603	$1.11 \pm 0.17$
30– $35^\circ$	$0.0041 \pm 0.0009$	0.00304	$1.35 \pm 0.35$

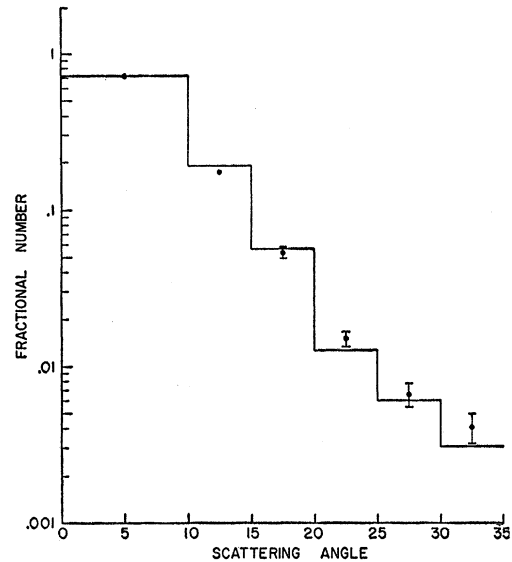
will be placed in the  $i$ th angular bin is

$$\int_{\Delta\Theta_i} P(\Theta, \theta) d\theta.$$

The total probability that a scattered mu will be placed in the  $i$ th bin is

$$N_{\text{th}}^i = \int_{\Delta\Theta_i} d\theta \int f(\Theta, t) P(\Theta, \theta) \Theta d\Theta.$$

The numbers  $N_{\text{th}}^i$ , calculated using the  $f(\theta, t)$  obtained in the section on multiple scattering, are listed along with the corresponding experimental numbers in Table I, and all of these results are plotted in Fig. 6. In Fig. 6  $N_{\text{th}}$  is plotted as a histogram whose height in a

FIG. 6. Angular distribution for  $\mu$  mesons scattered in bubble chamber.

particular angular interval is the fractional portion of the beam scattered into that interval. The experimental results, corrected for the scattered muons not visible in both chamber views, are shown as points placed in the middle of each angular interval.

The angular distribution of scattered  $\mu$  mesons expected on the basis of a purely Coulomb interaction with the lead atoms was calculated using the multiple scattering theory of Nigam, Sundaresan, and Wu.<sup>11</sup> This treatment of multiple scattering is a modification of the work of Molière<sup>12</sup> and Bethe<sup>13</sup> and is known to give good agreement with experiment for electron scattering from nuclei. The angular distribution is expressed in terms of  $f(\theta, t)$ , where  $f(\theta, t)\theta d\theta$  is the fraction of the beam scattered into the angular interval

<sup>11</sup> Nigam, Sundaresan, and Wu, Phys. Rev. **115**, 491 (1959).

<sup>12</sup> G. Molière, Z. Naturforsch. **3a**, 78 (1948).

<sup>13</sup> H. A. Bethe, Phys. Rev. **89**, 1256 (1953).

from  $\theta$  to  $\theta+d\theta$  by a scatterer of thickness  $t$ . The function  $f(\theta, t)$  is given by

$$f(\theta, t) = \int_0^\infty \psi d\psi J_0(\psi\theta) \times \exp \left\{ -Nt \int_0^\infty \sigma(x) x dx [1 - J_0(\psi x)] \right\},$$

for values  $\theta$  small compared to one radian. In this expression  $\sigma(x)$  is the differential scattering cross section of a lead atom,  $N$  is the number of scattering atoms per unit volume, and  $J_0(x)$  is the zero-order Bessel function. Bethe has shown that  $f(\theta, t)$  depends principally on the parameters  $x_e$  and  $x_a$ .  $x_e$  is essentially the nonangular dependent part of the single-scattering

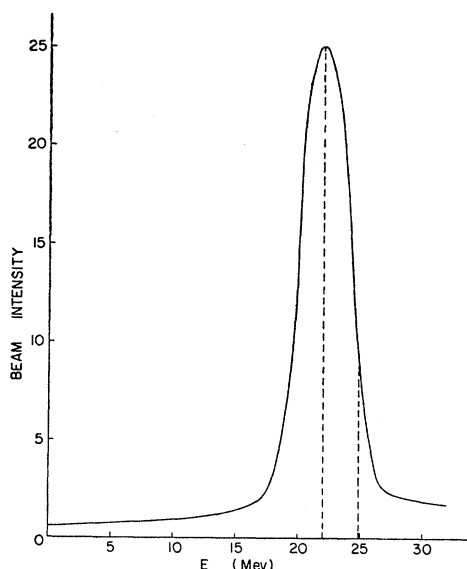


FIG. 7.  $\mu$ -meson differential range curve for counter experiment. Range of energies selected by final counter indicated by dashed lines.

probability and is given by

$$x_e^2 = 4\pi N t e^4 Z(Z+1) / (\bar{p}v)^2,$$

where  $\bar{p}$  is the momentum of the muon,  $v$  is its velocity, and  $Z$  is the atomic number of the scatterer.  $x_a$  is called the characteristic screening angle and is given in terms of  $q(x)$ , the ratio of the actual to the point charge cross section, by

$$-\ln x_a = \lim_{k \rightarrow \infty} \left\{ \int_0^k q(x) \frac{dx}{x} + \frac{1}{2} - \ln k \right\}.$$

In the application of the multiple-scattering theory to the bubble chamber setup, it was necessary to take account of the scattering both by the lead plate and by a  $\frac{3}{16}$ -in. layer of propane that was obscured from view by the Lucite plate holder. For the purpose of the calculation the lead and propane were assumed to be

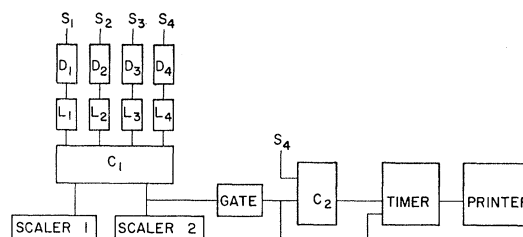


FIG. 8. Block diagram of electronics used in the counter experiment.

uniformly mixed, and furthermore, the propane was replaced by carbon with an effective  $Z$  of 6.2. With these assumptions it is easy to show that to a good approximation the multiple scattering is described by the  $f(\theta, t)$  above, provided that the  $x_e$  and  $x_a$  for the mixture are chosen according to

$$x_e^2 = x_{e1}^2 + x_{e2}^2,$$

and

$$x_a = x_{a1} U_1 x_{a2} U_2,$$

with  $U_1 = x_{e1}^2 / x_e^2$  and  $U_2 = x_{e2}^2 / x_e^2$ . Here the subscript 1 refers to the carbon and 2 to the lead.

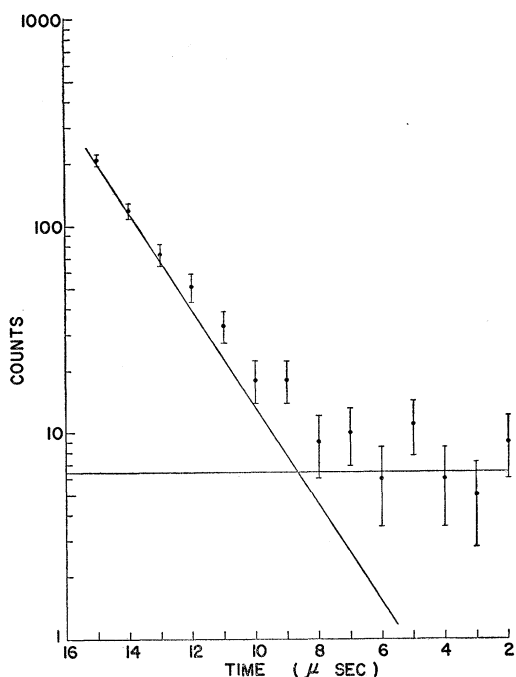
The results of the multiple-scattering calculation for the bubble chamber are shown in Table I. The numbers in the third column represent the fractions of the beam that are scattered into the angular intervals listed in the first column. The energy spectrum assumed for this calculation is the one shown in the differential range curve of Fig. 3.

#### COUNTER EXPERIMENT

For the counter experiment the energy spectrum of muons in the beam was the one shown in Fig. 7. The detector system used selected those in the interval defined by the dotted lines. The energy shown on the abscissa of the curve in Fig. 7 is the  $\mu$ -meson energy halfway through the lead plate as determined by the range-energy calculations of Willis and Thompson.<sup>8</sup>

For this work a beam was used which was composed of 75% electrons, 24%  $\mu^-$ , and 1%  $\pi^-$ . The incident beam was defined by a pair of counters placed 2 ft 11 in. apart as shown in Fig. 1(a). A lead collimator was placed between these counters to insure that the beam was parallel. The scattering target was a lead foil 0.022 in. thick and 4 in. in diameter mounted in a styrofoam holder. The analyzing telescope consisted of two counters separated by a sufficient amount of carbon to stop the  $\mu$ 's under study in the final counter. Counters 1, 2, 4 were 4-in. diam. by  $\frac{1}{4}$  in.; counter 3, 5-in. diam. by  $\frac{1}{4}$  in. All phototubes were 6810 A.

The electronics were as shown in Fig. 8. The coincidence circuit used had a resolution for full width at half maximum of 16  $\mu$ sec. A 4-fold coincidence started a delayed gate during which time additional counts in counter No. 4 were fed to the analyzing circuit. This circuit determined the time between

FIG. 9. Decay curve for  $\mu$  mesons in counter experiment.

the 4-fold coincidence and the following pulse by counting on a 10-Mc timing unit.

Detection was accomplished by the observation of the decay electron from the muon stopping in counter 4 after having traversed the telescope (1+2+3+4+delayed 4). Delayed electrons in the interval from 0.2 to 17  $\mu$ sec after the passage of a  $\mu$  meson were analyzed. The actual times recorded were the intervals between the decay electron and the end of the gate.

The use of a single counter to detect an electron originated within it resulted in high efficiency but imposed a limitation on the intensity that could be used without introducing accidental counts into the relatively long 17- $\mu$ sec gate. This was not significant in the scattered position where the counters could be shielded against accidental particles, and the true counting rate was of the order of 5 counts per hour, but caution had to be exercised during incident beam determinations.

The number of counts recorded per  $\mu$ sec fell off exponentially to a constant background with a half-life of the order of 1.3  $\mu$ sec as shown for the incident beam in Fig. 9. A weighted least-squares fit was made for each run to fit the curve  $y = Ae^{-\lambda t} + B$ . Here the parameter  $\lambda$  is assumed known and  $A$  and  $B$  are to be evaluated. If no interval contains zero counts,  $A$  is given by

$$A = \frac{(\sum_i e^{-\lambda t_i})[\sum_i (1/y_i)] - n[\sum_i (e^{-\lambda t_i}/y_i)]}{[\sum_i (1/y_i)][\sum_i (e^{-2\lambda t_i}/y_i)] - [\sum_i (e^{-\lambda t_i}/y_i)]^2}$$

with a standard deviation

$$\delta A = \left\{ \frac{\sum_i (1/y_i)}{[\sum_i (1/y_i)][\sum_i (e^{-2\lambda t_i}/y_i)] - [\sum_i (e^{-\lambda t_i}/y_i)]^2} \right\}^{\frac{1}{2}}$$

If one or more of the  $y_i$  are zero we make the following modification. Define  $p_i = 1/y_i$  if  $y_i \neq 0$ ;  $p_i = 1$  if  $y_i = 0$ . Then

$$A = \frac{[\sum_i (y_i p_i e^{-\lambda t_i})][\sum_i p_i] - [\sum_i (y_i p_i)][\sum_i (e^{-\lambda t_i} p_i)]}{[\sum_i p_i][\sum_i (e^{-2\lambda t_i}/p_i)] - (\sum_i e^{-\lambda t_i} p_i)^2}$$

$$\delta A = \left\{ \frac{\sum_i p_i}{(\sum_i p_i)[\sum_i (e^{-2\lambda t_i} p_i)] - [\sum_i (e^{-\lambda t_i} p_i)]^2} \right\}^{\frac{1}{2}}$$

The incident beam was determined by counting with counters 3 and 4 together with the carbon degrader placed immediately behind the lead target. The beam intensity was reduced to the level where counting losses and accidental coincidences were unimportant. The normalized rate calculated as outlined previously was  $(4200 \pm 210)$  counts/100 000 doubles.

TABLE II. Summary of results.

Angle (deg)	Effect plus background	Background	Cross section (barns)
28.25 R	1.81 $\pm$ 0.26	0.34 $\pm$ 0.23	14.14 $\pm$ 3.64
26.75 L	1.59 $\pm$ 0.23	0.36 $\pm$ 0.21	16.89 $\pm$ 4.08
27.5 Total			15.52 $\pm$ 2.73

The scattered beam was measured at 28.25° right and 26.75° left with equal numbers of counts taken scattered to each side. The designation “left” or “right” is defined with respect to the direction of motion of the beam. In every case runs were also made with the target removed to determine the stray background. The results are summarized in Table II.

The solid angle subtended by the counters at the target is  $\pi r_0^2/s^2$ , where  $s$  is the distance from the target to the counter. The effects due to the finite area of the target change this quantity by a factor of  $[1 - (9/16)(r_0^2/s^2)]$  which for the setup used amounted to 0.9989. The number of muons scattered to the counter  $N_0$  is given by

$$N_0 = N_i n \sigma (\pi r_0^2/s^2) \left( 1 - \frac{9 r_0^2}{16 s^2} \right),$$

where  $N_i$  is the number of muons incident on the target,  $n$  the number of scatterers per  $\text{cm}^2$ , and  $\sigma$  the cross section.

In our case this reduces to

$$\sigma = \frac{\text{scattered rate}}{\text{incident rate}} \times 4.794 \times 10^4 \text{ b.}$$

## RESULTS AND CONCLUSIONS

The final results of the bubble chamber experiment and the counter experiment are shown in Fig. 10. The ordinates show the ratios of the experimental fractions of mesons in the several angular intervals to the fractions calculated according to the theory of Nigam, Sundaresan, and Wu.<sup>4</sup> In the case of the counter measurement the ratio is based on a calculation made at the counter angle. The errors on the points are statistical. In addition it is estimated that the experimental numbers for the bubble chamber data could contain a systematic error of as much as  $\pm 10\%$  at  $22.5^\circ$  and as much as  $\pm 20\%$  at  $32.5^\circ$ . The uncertainties are principally in the meson energies, determined by their ranges in propane and in the correction factors to take account of scattered mesons that leave the chamber. For the counter data there is again an uncertainty in the energy that introduces a possible systematic error of  $\pm 10\%$ .

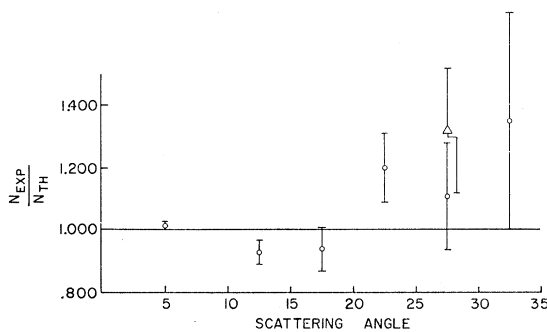


FIG. 10. Comparison of experimental and theoretical angular distribution for  $\mu$ -meson experiment. Circles indicate bubble chamber data. Triangle indicates counter point.

It should be pointed out that the calculations of Nigam, Sundaresan, and Wu are based on the single-scattering cross section of Dalitz,<sup>14</sup> which differs considerably in this case from the Rutherford cross section. This expression has been compared with a

<sup>14</sup> R. H. Dalitz, Proc. Roy. Soc. (London) **A206**, 509 (1951).

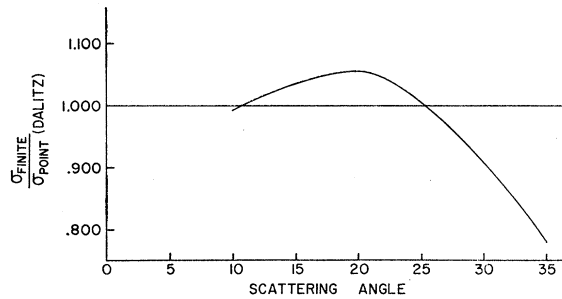


FIG. 11. Ratio of scattering cross section for finite nucleus to Dalitz cross section.

phase-shift calculation of Rawitscher<sup>15</sup> for a finite lead nucleus, and the comparison is shown in Fig. 11. The two differ by less than 5% for angles less than  $25^\circ$  at which point the finite nuclear size introduces a fairly rapid reduction in cross section. This reduction will raise the bubble chamber point at  $32.5^\circ$  in Fig. 10. The change will not be as great as the ratio of single-particle cross sections, however, because multiple and plural scattering are still important.

Considering the limitation on the accuracy in the experiment, the authors regard the agreement between theory and experiment to be satisfactory in spite of the slight experimental excess at larger angles. The momentum transfers investigated are not quite large enough to allow a distinction to be made between the point charge and the finite one, but within the range investigated there does not seem to be any evidence for an anomalous interaction between the  $\mu$  meson and the lead nucleus.

## ACKNOWLEDGMENTS

The authors wish to thank Richard Zener and Carlton Young for assistance during the early stages of this experiment. Walter Bertram and Edward Gray participated in several cyclotron runs, and the bubble chamber was loaned to us by Dr. Tom Fields and Dr. John Fetkovich.

<sup>15</sup> George Rawitscher (private communication). The authors are very grateful to Dr. Rawitscher for sending them his IBM-650 program to do these calculations. Responsibility for the correct use of this program, and hence for the accuracy of the curve in Fig. 11, rests with the authors of this paper.

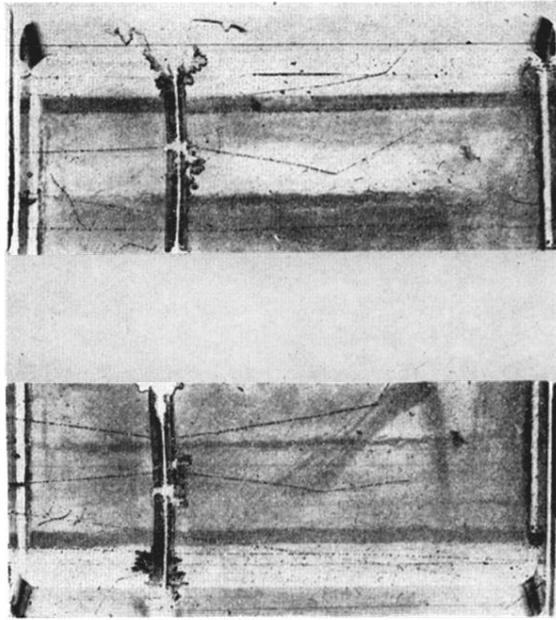


FIG. 4. Bubble chamber photographs of scattered  $\mu$  mesons.